STEM CELLS AND DEVELOPMENT
Volume 25, Number 9, 2016
Mary Ann Liebert, Inc.
DOI: 10.1089/scd.2015.0344

Mesangiogenic Progenitor Cells Derived from One Novel $CD64^{bright}CD31^{bright}CD14^{neg}$ Population in Human Adult Bone Marrow

Simone Pacini,[1] Serena Barachini,[1] Marina Montali,[1] Vittoria Carnicelli,[2] Rita Fazzi,[1] Paolo Parchi,[3] and Mario Petrini[1]

Mesenchymal stromal cells (MSCs) have been the object of extensive research for decades, due to their intrinsic clinical value. Nonetheless, the unambiguous identification of a unique in vivo MSC progenitor is still lacking, and the hypothesis that these multipotent cells could possibly arise from different in vivo precursors has been gaining consensus in the last years. We identified a novel multipotent cell population in human adult bone marrow that we first named Mesodermal Progenitor Cells (MPCs) for the ability to differentiate toward the mesenchymal lineage, while still retaining angiogenic potential. Despite extensive characterization, MPCs positioning within the differentiation pathway and whether they can be ascribed as possible distinctive progenitor of the MSC lineage is still unclear. In this study, we describe the ex vivo isolation of one novel bone marrow subpopulation (*Pop#8*) with the ability to generate MPCs. Multicolor flow cytometry in combination with either fluorescence-activated cell sorting or magnetic-activated cell sorting were applied to characterize *Pop#8* as $CD64^{bright}CD31^{bright}CD14^{neg}$. We defined *Pop#8* properties in culture, including the potential of *Pop#8*-derived MPCs to differentiate into MSCs. Gene expression data were suggestive of *Pop#8* in vivo involvement in hematopoietic stem cell niche constitution/maintenance. *Pop#8* resulted over three logs more frequent than other putative MSC progenitors, corroborating the idea that most of the controversies regarding culture-expanded MSCs could be the consequence of different culture conditions that select or promote particular subpopulations of precursors.

Introduction

Mesenchymal stromal cells (MSCs) have been the object of extensive research [1] for their intrinsic clinical value, due to multilineage differentiation capacity as well as involvement in hematopoiesis, immunoregulation, and growth factor/cytokine secretions [2–4]. A limitation is the very low number of cells in the tissue of origin that forced to use in vitro expansion protocols to achieve feasible amounts of cells for infusion or transplantation. However, there is increasing evidence that in vitro expansion induces drastic changes in phenotype and biological properties of MSCs, with significant possible implications for therapy [5–7]. Research aimed to shed light on MSC origin failed to identify an unambiguous unique in vivo progenitor, whereas the hypothesis that MSCs could possibly arise from different precursors is gaining consensus [8–11].

For a number of years our studies have focused on the optimization of MSC culture conditions suitable for clinical application. When fetal bovine serum (FBS) was replaced by autologous serum in cultures from human bone marrow (hBM), we noticed the emergence of a small population of cells with distinct morphology [12]. They presented rounded fried egg-like shape compared to the usual spindle-shaped morphology of MSCs, were highly refringent, showed firm plastic adherence after trypsin digestion, and retained angiogenic potential.

Notably, reverting to FBS-supplemented medium, MSC-like cells growing to confluence were obtained. We named this cell population mesodermal progenitor cells (MPCs) [12] for their in vitro characteristics of both mesenchymal and endothelial progenitor. Subsequently, we were able to define selective culture conditions, including commercial pooled human AB-type serum (PhABS) as supplement to

[1]Hematology Division, Department of Clinical and Experimental Medicine, University of Pisa, Pisa, Italy.
[2]Department of Surgical, Medical and Molecular Pathology and Critical Care Medicine, University of Pisa, Pisa, Italy.
[3]First Orthopedic Division, Department of Translational Research and New Technology in Medicine and Surgery, University of Pisa, Pisa, Italy.

generate MPCs at high grade of purity [13]. Our highly reproducible isolation protocol allowed the characterization of MPC morphological and biological properties.

MPCs showed to be nestin-positive, slow cycling, and Ki-67-negative, with chromosomes characterized by long telomeres. They expressed pluripotency-associated transcription factors Oct-4 and Nanog, at a difference with MSC master regulators Runx2 and Sox9 [14,15]. Phenotypically, MPCs expressed Endoglin (CD105) at a lower level than MSCs while lacking CD73, CD90, CD166, and the other markers typical of the mesenchymal phenotype [16]. They showed a different pattern of adhesion molecules with respect to standard cultured MSCs, being characterized by consistent expression of PECAM (CD31), integrins αL (CD11a), αM (CD11b), αX (CD11c), and particularly integrin β2 (CD18) that specifically sustain podosome-like structures.

MPCs rapidly differentiated into MSCs in standard commercial MSC expansion media, throughout an intermediate stage of differentiation activating Wnt5/Calmodulin cell signaling, replacing podosome-like structures, lowering adhesion on activated and nonactivated endothelium, and losing all angiogenic properties [17,18]. While the definition of specific MPC selective culture conditions allowed to definitively demonstrate the mesengenic and angiogenic potential of these cells, convincing data on MPC differentiation toward other mesodermal lineages are still lacking. Thus, we recently proposed a revision of the terminology, introducing a new definition of these cells as ''Mesangiogenic Progenitor cells,'' maintaining the acronym MPCs [19].

MPCs represent an attractive cell population with promising clinical applications. However, we believe that a detailed investigation about MPC origin in vivo is needed to identify putative precursors and to clarify MPC/MSC lineage relationship(s). In this study, we analyze the expression of MPC/MSC common antigen CD105 and differentially expressed antigen CD31 in ex vivo isolated hBM fractions. Integrating these results with multiparametric cell characterization, we managed to unambiguously describe a unique specific bone marrow subpopulation able to generate MPCs in selective culture conditions.

Materials and Methods

Immunomagnetic fractioning of hBM mononuclear cells

Donors and sample collection. The study has been performed according to the declaration of Helsinki and the local ethics committee of ''Azienda Ospedaliero-Universitaria Pisana'' approved the protocol for human bone marrow (hBM) blood sample collection. After written informed consent, hBM aspirates were obtained from 37 patients undergoing orthopedic surgery for hip replacement (13 M/14 F, median age 64). Briefly, a 20-mL syringe containing 500 I.U. of heparin was used to aspirate 10 mL of fresh bone marrow immediately after femoral neck osteotomy and before femoral reaming. Samples were processed soon after.

Isolation, fractioning, and plating of hBM mononuclear cells. Fresh bone marrow samples were diluted 1:4 in Dulbecco's modified phosphate-buffered saline (D-PBS; Life Technologies, Carlsbad, CA) and gently layered on Ficoll-Paque™ PREMIUM (GE Healthcare, Uppsala, Sweden). Samples were centrifuged at 400*g* for 25 min and hBM mononuclear cells (MNCs) were harvested at the interface, filtered on 50 μm filters, and washed twice in D-PBS. MSCA-1^{+} immunomagnetic depletion by the *Anti-MSCA-1* (*W8B2*) *MicroBeads Kit* (*human*) was performed on *autoMACS™ Pro Separator* (Miltenyi Biotec, Bergisch Gladbach, Germany), according to the manufacturer's instructions. MSCA-1^{neg} fraction was then incubated with *anti-CD105 MicroBeads* (*human*) (Miltenyi Biotec) and processed for separation running sensitive positive selection program.

The three fractions: MSCA-1^{+}, CD105^{+}MSCA-1^{neg}, and CD105^{neg}MSCA-1^{neg} were cytofluorimetrically evaluated for the expression of CD105, MSCA-1, and CD90. Aliquots were cytocentrifuged on glass slides to perform May–Grünwald–Giemsa stain and cultural properties were assayed in Dulbecco's modified Eagle's medium (DMEM)/10%PhABS and MesenPRO® RS (Life Technologies). To create permissive attaching conditions, cells were plated in tissue culture (TC) treated 24-well plates instead of using hydrophobic plastics as reported [13]. After 7 and 14 days of culture, wells were microscopically scanned by three independent operators and scored as follows: 0, no attached cells; 1, fewer than 20 cells/field; 2, 21–100 cells/field; 3, over 100 cells/field; and 4, cells at confluence. Scores were attributed considering either the MPC- or MSC-like morphology.

The same protocol was applied to obtain CD31^{+} fraction after MSCA-1 depletion, and morphological/cultural properties were assayed as above. Three further samples from donors (1 M/2 F, median age 64) were fractionated first performing monocytic/macrophagic and granulocytic lineage-positive cell depletion. hBM-MNCs were incubated with FITC-conjugated anti-*CD14* and anti-*CD66abc*e. Unbounded antibodies were removed by cell washing and anti-*FITC* MicroBeads-conjugated (Miltenyi Biotec) antibodies applied for depletion on *autoMACS Pro Separator*, according to the manufacturer's instructions. CD14/CD66^{neg} fraction was then incubated with anti-*CD31* PE and, after cell washing, incubated with anti-*PE* MicroBeads-conjugated and processed for sensitive positive selection. The three fractions, CD14/CD66^{+}, CD31^{+}CD14^{neg}CD66^{neg}, and CD31^{neg}CD14/CD66^{neg}, were then processed as described above.

Multicolor flow cytometry analysis of hBM-MNCs

Donors. Freshly isolated hBM-MNCs from 20 donors (10 M/10 F, median age 65) were processed for seven-color flow cytometry analysis, incubating cells for 30 min at 4°C with a set of fluorochrome-conjugated antibodies. After cell washing with *MACS*Quant Running Buffer (Miltenyi Biotec), samples were acquired on *MACS*Quant Flow Cytometer (Miltenyi Biotec) and analyzed by *MACS*Quantify Analysis Software (Miltenyi Biotec). Unstained and FMO (fluorescence minus one) tests were also processed to set gates for the analysis.

Antibodies. Antibodies anti-*CD31* PE-Cy7, anti-*CD18* PE or APC, anti-*CD51* FITC, anti-*CD64* FITC, anti-*CD14* FITC, PE or PerCP-Cy5.5, anti-*CD66abce* FITC, anti-*CD34* VioBlue®, anti-*CD38* FITC, anti-*CD44* PE, anti-*CD45* VioBlue® or APC-Vio770, anti-*CD3* FITC or PerCP-Cy5.5, anti-*CD20* FITC or PerCP-Cy5.5, anti-*CD15* FITC, anti-*CD16* PerCP-Cy5.5, anti-*HLA-DR* VioBlue®, anti-*CD86*

VioBlue®, anti-*CD80* VioBlue®, anti-*CD90* FITC and PerCP-Cy5.5, anti-*CD133* APC, anti-*CD138* PE, anti-*CD140a* PE, anti-*CD146* FITC, and anti-*MSCA-1* PE were from Miltenyi Biotec. Anti-*STRO-1* AlexaFluor® 647, anti-*CD73* PE-Cy7, anti-*CD105* PerCP-Cy5.5, anti-*CD140b* PE, anti-*CD56* APC, anti-*CD309* PerCP-Cy5.5, anti-*CD115*, anti-*CD144* PE, anti-*SSEA-3* FITC, and anti-*SSEA-4* FITC were from BioLegend (San Diego, CA). Anti-*CD27*1 PE, anti-*CD11b* PE, anti-*CD11c* PE, and anti-*CD36* APC were from BD Biosciences (San Jose, CA).

Fluorescence-activated cell sorting of hBM-MNCs

hBM-MNCs were stained with anti-*CD18 PE*, anti-*CD31* PE-Cy7, and a cocktail of FITC-conjugated antibodies, including anti-*CD3*, anti-*CD20*, anti-*CD14,* and anti-*CD66abce*. After 30 min at 4°C cells were washed with prerefrigerated autoMACS Running Buffer and processed for cell sorting on S3™ Cell Sorter (Bio-Rad, Hercules, CA) equipped with ProSort® Software (Bio-Rad) applying ''Purity'' sort mode. Sorted cells were then cytocentrifuged on glass slides to perform May Grünwald–Giemsa and cytochemical staining or alternatively plated in DMEM/10%PhABS using TC 24-well plates. After 5 days of culture, cells were exposed to mesengenic and angiogenic differentiating conditions, tested for acetylated low-density lipoprotein (Ac-LDL) uptake and phagocytosis, or detached by TrypLE Select® (Life Technologies) digestion, and analyzed by flow cytometry, as described below.

Nestin detection was performed on sorted cells seeded in two-well Lab-Tek Permanox® Chamber Slides (Thermo Fisher Scientific, Waltham, MA). Fluorescence-activated cell sorting (FACS) was extended to hematopoietic lineage antigens using a cocktail of *CD64*-FITC, *CD31*-PE/Cy7, and *CD14*-PE antibodies. Within CD64^{bright}CD31^{bright} population, CD14^{neg} and CD14^{+} cells were separated on S3 Cell Sorter and processed as described above.

Cell cultures

MPC selective cultures. Freshly sorted cells underwent MPC-selective culture in DMEM supplemented with 1% of GlutaMAX®, penicillin and streptomycin (Life Technologies), and 10% of PhABS of U.S. origin from Lonza (Walkersville, MD). Cultures were maintained at 37°C and 5% CO_2 for 5–6 days. Cells were then harvested by TrypLE Select digestion and applied for cell characterization and differentiation potential evaluation, as described below.

Mesengenic differentiation. To induce differentiation into MSCs, freshly sorted cells and the MPCs derived from them were first cultured for 7 days in MesenPRO Reduced Serum (RS) Medium (Life Technologies), and then terminally differentiated into adipocytes and osteocytes using StemMACS® AdipoDiff and StemMACS® OsteoDiff Media from Miltenyi Biotec, respectively, for 21 days. Media were refreshed every 48 h. In parallel, cells were detached by TrypLE Select digestion and washed twice in *MACS*Quant Running Buffer (Miltenyi Biotec) for flow cytometry.

Angiogenic differentiation assessment of sprouting angiogenesis in three-dimensional culture. Three-dimensional (3D) spheroids were generated by the hanging drop method [20,21] with 1.5×10^5 of sorted cells or CD64^{bright}CD31^{bright}CD14^{neg}-derived MPCs per drop and incubated overnight at 37°C in 5% CO_2 for cell aggregation. Spheroids were then gently applied onto Matrigel® thick gel layer and cultured in EGM-2 medium. Sprouting was evaluated after 24 h and after 7 days by measuring the distance between last invading cell and the spheroid edge. Thereafter, Matrigel was melted incubating 3D cultures at 4°C for 2 h and diluted 10 mL of prerefrigerated D-PBS. Spheroids were harvested by centrifugation at 150*g* and enzymatically dissociated by adding TrypLE Select to obtain single cell suspensions, and standard capillary-like tube (CLT) formation assay was then performed on these cells [22].

Hematopoietic colony-forming assay. From 1.5×10^5 to 2.0×10^5 of freshly sorted CD64^{bright}CD31^{bright}CD14^{neg} and CD64^{bright}CD31^{bright}CD14^{+} were seeded in 4 mL of StemMACS® HSC-CFU medium (Miltenyi Biotec). Using a sterile 1-mL syringe fitted with a 16-gauge blunt-end needle, the suspension was mixed and an aliquot of 2 mL was put into two 35-mm Petri dishes. Cultures were incubated at 37°C and 5% CO_2 for 12 to 14 days.

Mononuclear phagocyte differentiation. Freshly sorted CD64^{bright}CD31^{bright}CD14^{neg} cells were seeded 2×10^4 cells/cm^2 in 24-well plates and cultured in DMEM/10%PhABS with or without 50 ng/mL of human recombinant granulocyte/macrophage colony-stimulating factor (hGM-CSF), for 5–6 days. At the end of the culture time, media were replaced by fresh DMEM/10%PhABS and 10 μL/mL of Indian ink were added. Cultures were incubated at 37°C and 5% CO_2 for additional 4 h, extensively washed with fresh culture medium, and put back into the incubator. The day after, bright-field microscopic pictures were taken applying inverted DM IRB Leica microscope (Leica, Wetzlar, Germany), equipped with LAS image acquisition software (Leica).

Cell and culture characterization

Morphological and cytochemical staining. Morphological May Grünwald–Giemsa staining was performed on Wescor Aerospray® 7120 automatic slide stainer (ELITech Group, Puteaux, France). Cytochemical staining was carried out by α-naphthyl acetate esterase and the Tartrate-Resistant Acid Phosphate (TRAP) Detection Kit (Sigma-Aldrich, Saint Louis, MO), according to the manufacturer's instructions, and counterstained with Gill's Hematoxylin. Peroxidase activity was revealed by benzidine oxidation [23] and slides counterstained by Giemsa reagent diluted 1:10.

Flow cytometry characterization of cultured cell populations. Freshly isolated MPCs and differentiated MSCs were processed for flow cytometry analysis, incubating cells for 30 min at 4°C with a set of fluorochrome-conjugated antibodies, including: anti-*CD31* PE-Cy7, anti-*CD18* APC, anti-*CD14* FITC, anti-*CD66abce* FITC, anti-*CD34* VioBlue, anti-*CD90* FITC, anti-*CD146* FITC, and anti-*MSCA-1* PE were from Miltenyi Biotec. Anti-*STRO-1* AlexaFluor 647, anti-*CD73* PE-Cy7, and anti-*CD105* PerCP-Cy5.5 were from BioLegend. The anti-*CD11c* PE antibody was from BD Bioscience. After cell washing with *MACS*Quant Running Buffer (Miltenyi Biotec), samples were acquired on *MACS*Quant Flow Cytometer (Miltenyi Biotec) and analyzed by *MACS*Quantify Analysis Software (Miltenyi Biotec). Proper isotype controls (all from Miltenyi Biotec) were also employed to set the positive regions of the histograms.

Lipid droplet accumulation. Cells were cultured under adipogenic conditions, medium removed, and wells washed twice with prewarmed D-PBS. Cells were then incubated with 200 nM Nile Red (Life Technologies) for 10 min at 37°C in the dark.

Calcium deposits. Osteogenic induced cultures were processed by the OsteoImage™ Mineralization Assay Kit (Lonza), according to the manufacturer's instructions. Wells were washed twice with D-PBS and pictures taken using the inverted fluorescence DM IRB Leica microscope (Leica), equipped with LAS image acquisition software (Leica).

Nestin detection. Cells in chamber slides were fixed for 15 min in 4% paraformaldehyde solution and subsequently permeabilized by 0.05% Triton X-100 for 30 min. Immunofluorescence was carried out using mouse monoclonal antibodies against Nestin (Abcam, Cambridge, United Kingdom) and the Goat Anti-Mouse SFX Kit (Life Technologies), according to the manufacturer's instructions, using AlexaFluor® 488 anti-mouse IgG. Slides were then stained with Phalloidin AlexaFluor® 555-conjugated (Life Technologies) for 30 min to reveal F-actin organization. Nuclei were detected by ProLong® Gold Antifade Reagent with 4′,6-diamidino-2-phenylindole (DAPI; Life Technologies).

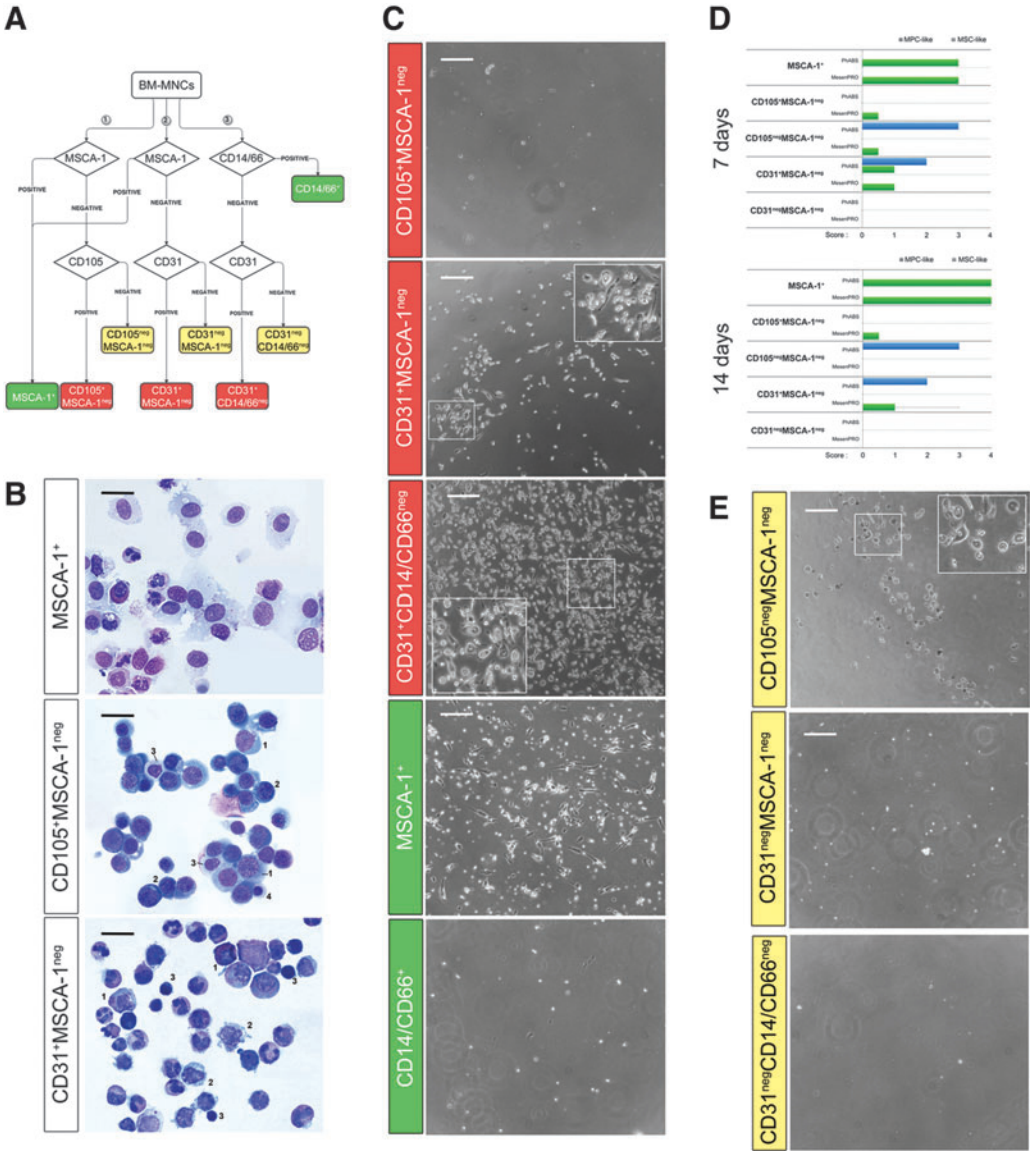

FIG. 1. Morphological characterization of hBM-MNC immunomagnetic fractions. Two-step immunomagnetic hBM-MNC cell separation gave rise to six fractions, including $CD105^{+}MSCA\text{-}1^{neg}$, $CD31^{+}MSCA\text{-}1^{neg}$, $CD31^{+}CD14^{neg}CD66^{neg}$ (*red boxes* in **A**), double negative fractions (*yellow boxes* in **A**), $MSCA\text{-}1^{+}$-positive control, and $CD14/66^{+}$-negative control (*green boxes* in **A**). May Grünwald–Giemsa staining of $MSCA\text{-}1^{+}$-positive control revealed the cell stromal appearance. $CD105^{+}$ fraction included erythroid elements as pronormoblasts (1), basophilic (2), polychromatophilic (3), and orthochromic (4) normoblasts. $CD31^{+}MSCA\text{-}1^{neg}$ fraction appeared to be constituted by myeloid (1), monocytoid (2), and lymphoid (3) elements (**B**, *black* scale bar: 50 μm). Under MPCs/MSCs permissive culture conditions, at day 7 MPC-like cells were detected in $CD31^{+}$ fractions, as well as in the $CD105^{neg}MSCA\text{-}1^{neg}$ (**C**–**E**, *white* scale bar: 200 μm). hBM-MNC, human bone marrow mononuclear cell; MPCs, mesodermal progenitor cells; MSCs, mesenchymal stromal cells.

Pictures were taken using standard fluorescence DM RB (Leica) and LAS AF image acquisition software (Leica).

Ac-LDL uptake. Cultures of MPCs from CD64^{bright} CD31^{bright}CD14^{neg} population were incubated for 4 h at 37°C with 5 μg/mL AlexaFluor 488-conjugated Ac-LDL (Life Technologies) in DMEM/1% bovine serum albumin. Cells were then washed twice and pictures taken as described above using inverted fluorescence microscope.

Gene expression analysis

Samples of FACS sorted CD64^{bright}CD31^{bright}CD14^{neg} and CD64^{bright}CD31^{bright}CD14^{+} cells from seven patients (3 M/4 F, median age 63), together with five samples of MPC cultured cells were processed for gene expression analysis of *PECAM*, *NESTIN, SPP1, NANOG,* and *OCT-4A* (NCBI Gene: NM_000442, NM_006617, NM_001040060, NM_024865, and NM_002701). Total RNA was extracted using the RNeasy Micro Kit (Qiagen GmbH, Hilden, Germany) according to the manufacturer's instructions. One hundred nanograms of RNA samples were retrotranscribed applying the QuantiTect Reverse Transcription Kit (Qiagen GmbH) and 2 μL samples of 10-fold cDNA dilutions were amplified by quantitative real-time polymerase chain reaction, using iCycler-iQ5 Optical System (Bio-Rad) and SsoAdvanced SYBR Green SuperMix (Bio-Rad). Samples were run in duplicate.

All primer pairs (Supplementary Table S1; Supplementary Data are available online at www.liebertpub.com/scd) were from Sigma-Aldrich. Relative quantitative analysis was performed following $2^{-\Delta\Delta Ct}$ Livak method [24]. Normalization was performed by using *GAPDH* and *ATP5B* (NCBI Gene: NM_002046 and NM_001686) housekeeping genes. Statistical analysis was carried out by two-tailed *t*-test, and results were reported as mean ± standard deviation.

Results

MPC progenitors were found in a specific CD31^{+} fraction from hBM-MNCs

Two-step immunomagnetic hBM-MNC cell separation allowed us to obtain three different fractions expected to include MPC progenitors: CD105^{+}MSCA-1^{neg}, CD31^{+} MSCA-1^{neg}, and CD31^{+}CD14/CD66^{neg} (red boxed in Fig. 1A). Cell cultures were also set up from MSCA-1^{+} MSC progenitors as positive control, whereas CD14/66^{+} fraction was deemed as negative control (green boxed in Fig. 1A). Double negative cell fractions were also taken in consideration and assayed throughout the experiments (yellow boxed in Fig. 1A).

MSCA-1^{+} fraction showed a percentage of CD105^{+} MSCA-1^{+}CD90^{bright} cells of 56.6% ± 4.3% ($n=7$). This population was characterized by very large cells with abundant faint cytoplasm, large regular elliptical nuclei showing finely dispersed chromatin with nucleoli occasionally evident. Significant leukocyte contamination was observed. Conversely, CD105^{+}MSCA-1^{neg} fraction was exclusively constituted by CD105^{+}MSCA-1^{neg}CD90^{neg} cells (97.5% ± 1.6%; $n=4$) showing different morphologies very similar to the progenitors of the erythroid lineage, from pronormoblasts to orthochromic normoblasts. CD31^{+}MSCA-1^{neg} fraction (purity: 97.7% ± 2.7%, $n=4$) featured a large variety of myeloid progenitors, elements of monocytic/macrophagic appearance, and cells from the lymphoid lineage (Fig. 1B). CD31^{+}CD14/CD66^{neg} cells (purity: 96.8% ± 3.4%, $n=4$) resulted highly similar to the CD31^{+} cells obtained after MSCA-1 depletion, with a mild but evident increase of the lymphoid counterpart (data not shown).

CD105^{+}MSCA-1^{neg} cells cultured under MPC-selective conditions showed complete lack of adherence to plastic and were easily washed out at media change. Conversely, after 7 days under MPC-selective culture conditions, MSCA-1-depleted CD31^{+} cells showed strong adherence, with over 20 rounded refringent MPC-like cells/field detected (median score = 2, $n=3$, Fig. 1C, blue bars in Fig. 1D) with score unvaried within 14 days of culture (Supplementary Fig. S1A). In DMEM/10%PhABS CD31^{+}CD14/CD66^{neg} fraction generated considerably more MPC-like cells as compared with CD31^{+}MSCA-1^{neg} fraction (median score = 4, $n=3$). Among double negative populations, more than 100 MPC-like cells per microscopic fields were detected, after 7 days, only in the CD105^{neg}MSCA-1^{neg} fraction cultured in DMEM/10%PhABS (median score = 3, $n=4$, Fig. 1D, E). Cells maintained vitality at day 14 of culture without signs of proliferation (Supplementary Fig. S1A). MPC-like cells generated from both CD31^{+}MSCA-1^{neg} and CD105^{neg}MSCA-1^{neg} were able to differentiate into MSC-like cells when DMEM/10%PhABS was replaced with MesenPRO RS and culture extended for further 14 days (Supplementary Fig. S1B).

After 7 days of culture of MSCA-1^{+} fraction in DMEM/10%PhABS, attached, flat multibranched cells were detected (Fig. 1C, D). These slightly proliferating cells were subconfluent at day 14, with evident signs of spontaneous mesengenic differentiation (Supplementary Fig. S1C). As expected, negative control population CD14/CD66^{+} was never able to generate adherent cultures (Fig. 1C).

When bone marrow-derived cell fractions were cultured directly in MesenPRO RS medium, confluent MSC-like spindle-shaped cells were obtained only from MSCA-1^{+} fraction (median score = 3, $n=7$ after 7 days, median score = 4, $n=7$ after 14 days; Fig. 1D and Supplementary Fig. S1D, E). Those cells were able to differentiate toward the mesengenic lineage after culturing in StemMACS OsteoDiff or StemMACS AdipoDiff medium (data not shown), confirming their MSC nature.

Few attached cells of undefined morphology were found when seeding CD105^{neg}MSCA-1^{neg} (median score = 0.5, $n=4$) and CD31^{+}MSCA-1^{neg} (median score = 1, $n=3$) cells in MesenPRO RS medium (Fig. 1D). Those small condensed cells showed neither MPC-like nor MSC-like features and remained firmly attached without a sign of proliferation. Therefore, they were considered negative.

In conclusion, positive selection for markers CD105 and MSCA-1 did not allow isolation of *bona fide* MPC precursors that appear to reside specifically in CD31^{+}CD14^{neg} CD66^{neg} fraction.

A specific CD31^{+} subpopulation generated MPCs in culture

Immunomagnetic selection experiments indicated that CD31^{+} fraction was the candidate for further investigation. To analyze the large CD31^{+} bone marrow compartment

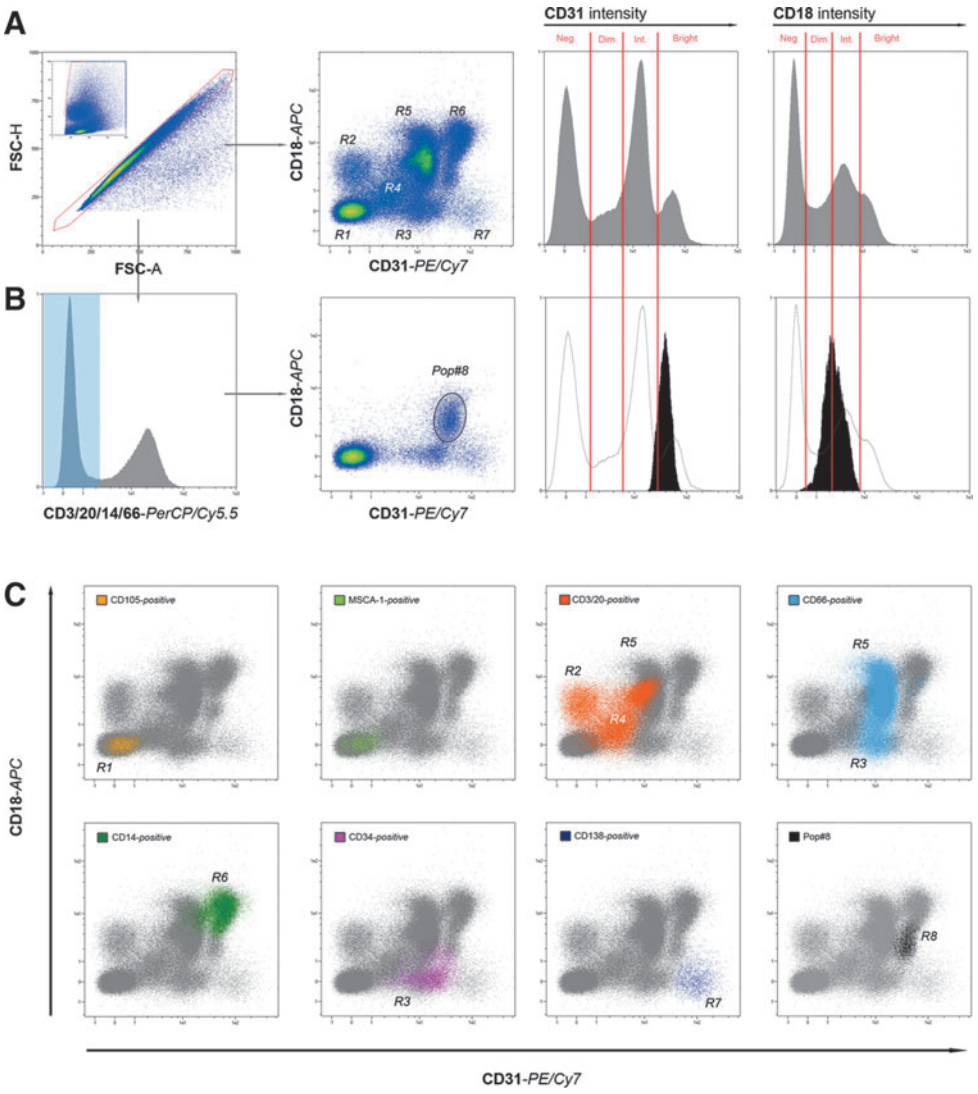

FIG. 2. *Pop#8* identification by lineage exclusion. Applying multicolor flow cytometry of freshly isolated hBM-MNCs, events generated by single cells were selected on the basis of scatter signals and plotted on CD18 versus CD31 density plot. Seven regions were identified (R1–R7) according to a combination of four levels of CD31/CD18 intensity: *Neg* (negative), *Dim* (low level of expression), *Int* (intermediate level of expression), and *Bright* (high level of expression) **(A)**. Gating on lineage-negative cells (not expressing CD3, CD20, CD14, or CD66), CD18 versus CD31 density plot revealed in all samples a residual $CD31^{bright}CD18^{dim/int}$ population that we defined as unknown population #8 (*Pop#8*) **(B)**. Backgating strategy showed that most of the well-acquainted hBM populations, such as $CD105^{+}$ (*yellow dots*), $MSCA\text{-}1^{+}$ (*light green dots*), mature lymphocytes (*orange dots*), granulocytes (*light blue dots*), HSCs (*pink dots*), and plasma cells (*violet dots*) occupied one or more of the expected R1–R7 regions **(C)**. Conversely, *Pop#8* (*black dots*) occupied one distinct region (R8). HSCs, hematopoietic stem cells.

seven-color flow cytometry was carried out using specific markers. In particular, Integrin-β_2 (CD18) is known to be highly expressed on the surface of MPCs isolated in culture [17], although widely distributed within the hematopoietic compartment in vivo. CD31 and CD18 both results expressed nonhomogeneously, and we scored samples at four different levels: *negative*, *dim, intermediate,* and *bright* (Fig. 2A). CD18 versus CD31 plotting cytogram allowed the identification of eight distinct regions (R1–R8) of even distribution (Table 1 and Fig. 2A). Extending the analysis of CD18 versus CD31 plotting cytogram to specific bone marrow subpopulations (Table 2), we gated the experiments for the expression of lineage-specific markers (Supplementary Fig. S2A).

As expected, $CD105^{+}$ and $MSCA\text{-}1^{+}$ cells were detected within the $CD31^{neg}CD18^{neg}$ region (*R1*). Lymphocytes and

TABLE 1. EVENTS DISTRIBUTION IN CD31 VERSUS CD18 DOT PLOTS

Region	*Populations*	*CD31 intensity*	*CD18 intensity*
R1	MSCs and erythroid progenitors	Negative	Negative
R2	Subpopulation of lymphoid cells	Negative	Dim
R3	HSCs, EPCs, small subpopulation of myeloid cells	Intermediate	Negative
R4	Subpopulation of lymphoid cells	Dim	Intermediate
R5	Most of myeloid cells	Intermediate	Bright
R6	Monocytoid cells and macrophages	Bright	Bright
R7	Plasmacells	Bright	Negative
R8	*Pop#8*	Intermediate–bright	Intermediate

Eight separate regions were identified and characterized by combinations of CD31 and CD18 intensity of expression.
EPCs, endothelial precursor cells; HSCs, hematopoietic stem cells; MSCs, mesenchymal stromal cells.

Table 2. Distinct hBM Subpopulations Occupied Different Regions in CD18 Versus CD31 Plot

Population	*Lineage marker*	*Region*	*CD31 intensity*	*CD18 intensity*
Mesenchymal/erythroid	CD105$^+$	R1	Negative	Negative
BM-MSCs	MSCA-1$^+$	R1	Negative	Negative
Lymphoid	CD3/CD20$^+$	R2, R4, R5	Negative–dim–intermediate	Dim–intermediate–bright
Myeloid	CD66$^+$	R3, R5	Intermediate	Negative–bright
Monocytoid	CD14$^+$	R6	Bright	Bright
Plasmacytoid	CD138$^+$	R7	Bright	Negative
HSCs/EPCs	CD34$^+$	R3	Intermediate	Negative
Pop#8	Lin^{neg}CD34^{neg} CD31$^+$CD18$^+$	R8	Bright–	Dim–intermediate

Distribution of hBM subpopulations as defined by specific immunophenotypes resulted specific with the exception of lymphocytes that segregated into three different regions and myeloid cells that spread seamlessly from R3 to R5.
BM-MSCs, bone marrow–mesenchymal stromal cells; hBM, human bone marrow.

their precursors, marked by the expression of CD3 or CD20, were mainly distributed among CD31^{neg}CD18^{dim} (*R2*), CD31^{dim}CD18^{int} (*R4*), and CD31^{int}CD18^{bright} (*R5*). Myeloid CD66$^+$ cells mostly resulted in CD31^{int}CD18^{bright} (*R5*), a small percentage was characterized by fading CD18 intensity, and a subpopulation was CD18^{neg} (*R3*). The monocytic–macrophagic lineage, marked for the expression of CD14, occupied exclusively the CD31^{bright}CD18^{bright} region (*R6*), whereas hematopoietic stem cells (HSCs) and endothelial precursor cells (EPCs), both CD34$^+$ cells, were plotted in *R3*. The remaining CD31^{bright}CD18^{neg} (*R7*) rare population revealed almost exclusively constituted by CD138$^+$ elements, ascribable to normal bone marrow plasma cells (Supplementary Fig. S2A and Fig. 2C).

Gating on lineage-negative cells (CD34^{neg}, CD3/20^{neg}, CD14^{neg}, and CD66^{neg}, HSCs/EPCs CD18^{neg} populations and plasma cells) CD18 versus CD31 density plot, revealed in all samples, a residual CD31^{bright}CD18$^{dim/int}$ population we defined as ''unknown population #8'' (*Pop#8*) (Fig. 2B), this population resulted around 1% of the total BM-MNCs ($1.27\% \pm 0.60\%$; $n = 17$) without significant variations, related to donor's age or sex. Backgating revealed a separated and specific region for *Pop#8* on the plot (*R8*), adjacent to the monocytoid, myeloid, and CD34$^+$ populations (Fig. 2C). To the best of our knowledge, a population with similar features has not been characterized yet. *Pop#8* is the only CD31$^+$/CD18$^+$ population not attributable to any of the main bone marrow subpopulations. Therefore, it appeared to be a reasonable candidate to represent the ex vivo progenitor of MPCs.

To verify our hypothesis, FACS sorting was performed on freshly isolated hBM-MNCs after incubation with FITC-conjugated anti-CD3/CD20/CD14/CD66abce, PE-conjugated anti-CD18, and PE-Cy7-conjugated anti-CD31. *Pop#8* sorting protocol included in hierarchical order: (1) selection of cellular events on forward scatter (FSC) versus side scatter (SSC) plot, (2) selection of single-cell events on FSC-A versus FSC-H plot, (3) exclusion of FITC-positive events, and (4) selection of CD31^{bright}CD18$^{dim/int}$ events on PE versus PE-Cy7 plot, excluding HSCs/EPCs in R3, and plasma cells in R7. CD3/20/14/66$^+$ cells were sorted in parallel, as control. *Pop#8* (median purity of $97.4\% \pm 1.6\%$, $n = 6$) was the only population able to generate adherent MPC-like cells, characterized by the typical MPC fried egg-shape shown in PhABS cultures (Fig. 3A, B). *Pop#8* differentiation potential was tested and derived cultured cells were definitively characterized as MPCs for the presence of a high number of dispersed podosomes, positive stain for Nestin (Fig. 3C), and typical MPC CD31$^+$, CD18$^+$, and CD11c$^+$ immunophenotype (Fig. 3D).

Moreover, *Pop#8*-derived MPCs showed the ability to differentiate into MSCs once switched from DMEM/10% PhABS to MesenPRO RS medium, consistently with MPCs isolated by plastic adherence [18]. After 7 days of mesengenic differentiation, cells expressed MSC-associated markers CD105, CD90, CD73, STRO-1, and MSCA-1, whereas CD31, CD18, and CD11c expression was rapidly lost during differentiation (Fig. 3E). Typical spindle-shaped fibroblastoid cell morphology was evident as well as the ability to reach confluence within a week (Fig. 3F). F-actin resulted reorganized in the characteristic stress fibers usually reported in MSCs, whereas podosome-like structures were lost. Moreover, differentiation was associated to reduced nestin expression (data not shown).

MSC typical features of differentiated cultures were further confirmed by inducing terminal differentiation into adipogenic or osteogenic lineages. After 21 days under adipogenic stimuli, lipid droplet accumulation was easily detectable by red fluorescence, whereas osteogenic stimuli led to high deposition of mineralized matrix, revealed by intense green florescence (Fig. 3G, upper panels). On the other side, cultures kept in MesenPRO RS medium for 21 days showed no spontaneous differentiation (Fig. 3G, lower panels).

Characterization of Pop#8

May Grünwald–Giemsa staining of freshly sorted *Pop#8* showed distinctive morphological features. Cells were 30–40 μm in diameter with abundant densely basophilic cytoplasm sometimes revealing intense dot-patterned acidophilic stain. Nuclei appeared of regular shape with condensed chromatin, rarely showing mild invaginations. Evident nucleoli were frequently found (Supplementary Fig. S3A). All other CD31 versus CD18 plot cell populations revealed the morphologies expected for related lineages (Supplementary Fig. S2B). *Pop#8* retained high peroxidase activity (dark brown in Supplementary Fig. S3B), from very low to absent

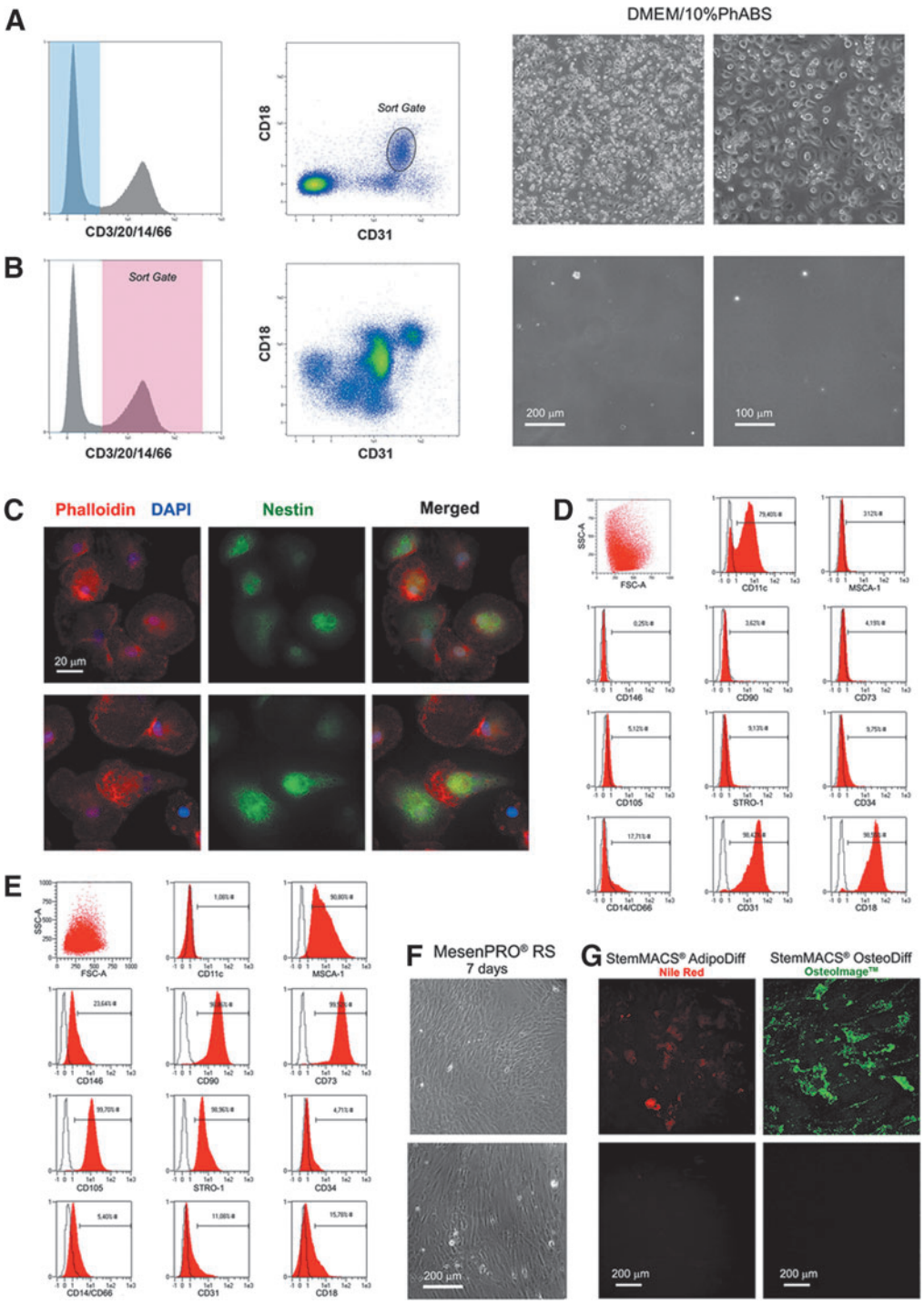

FIG. 3. *Pop#8* exclusive in vitro generation of MPCs. After 5 days in MPC-selective culture conditions (DMEM/10%PhABS) *Pop#8* generated MPC-like cells characterized by the peculiar fried egg-shaped morphology **(A)**. CD3/20/14/CD66^{+} cells were sorted in parallel, as control population **(B)**. Immunofluorescence analysis of *Pop#8*-derived MPCs, revealed podosome-like actin organization (*red* in **C)** and intense positivity to nestin (*green* in **C**). The MPC phenotype was confirmed by flow cytometry **(D)**. After 7 days of culture under mesengenic-differentiating conditions (MesenPRO® RS medium), *Pop#8*-derived MPCs gave rise to confluent cells showing MSC phenotype **(E)** and morphology **(F)**. To confirm the mesenchymal nature of *Pop#8* MPC-derived MSCs, cultures were further exposed to adipogenic or osteogenic stimuli. Lipid droplet (*red* in **G)** accumulation and calcium deposition (*green* in **G**) were detected only in terminally differentiated cultures **(G**, *upper panels*). No fluorescence signals were detected in cultures maintained in MesenPRO RS medium **(G)** (*lower panels*). DMEM, Dulbecco's modified Eagle's medium; PhABS, pooled human AB-type serum; RS, reduced serum.

TABLE 3. POP#8 IMMUNOPHENOTYPE

A		B	
Antigen	*Intensity*	*Antigen*	*Intensity*
CD34	Negative	*CD11b*	Neg/dim
CD44	Bright	*CD11c*	Negative
CD51	Negative	*CD13*	Neg/dim
CD56	Negative	*CD14*	Negative
CD105	Negative	*CD15*	Negative
CD133	Negative	*CD16*	Negative
CD140a/b	Negative	*CD33*	Positive
CD144	Negative	*CD36*	Negative
CD146	Negative	*CD38*	Positive
CD271	Negative	*CD45*	Dim
CD309	Negative	*CD64*	Bright
STRO-1	Negative	*CD80*	Negative
SSEA-3	Negative	*CD86*	Negative
SSEA-4	Negative	*CD115*	Negative
		HLA-DR	Positive

naphthyl-acetate esterase activity, and absent tartrate-resistant acid phosphatase activity, as shown by cytoenzymatic assays.

Immunophenotyping showed that none of the antigens mostly applied for perspective isolation of MSCs was expressed in *Pop#8* (Table 3A). In detail, *Pop#8* showed no expression of CD105 and MSCA-1 antigens, thus confirming the results from the immunomagnetic selection; no expression of CD271 (LNGFR), STRO-1, SSEA-3, SSEA-4, or CD146 (MCAM), as well as platelet-derived growth factor receptor chains (CD140a, CD140b) or Integrin αV (CD51). Moreover, *Pop#8* did not express common endothelial-associated antigens CD309 (KDR), CD144 (VE-cadherin), alongside to CD34 and CD133 (Supplementary Fig. S3C and Table 3A). MPC highly expressed CD11c (Integrin αX) and CD11b (Integrin αM) were not found in *Pop#8*, but they were rapidly induced in DMEM/10%PhABS culture (Supplementary Fig. S3C and Fig. 3D).

Immunophenotype analysis extended to the hematopoietic lineage antigens revealed low levels of CD45 and intense positivity for the myeloid marker CD64 (Table 3B). Thus, events were gated for bright expression of both CD31 and CD64. Within this population most cells showed to be either definitely CD14^{+} or CD14^{neg}, with only a small portion of cells expressing CD14 at intermediate levels. In CD18 versus CD31 cytogram, the CD64^{bright}CD31^{bright}CD14^{neg} population (1.38% ± 0.30%; $n = 11$), plotted exclusively in the *R8* region associated to *Pop#8* cells (Fig. 4A). In CD45 versus SSC cytogram, CD64^{bright}CD31^{bright}CD14^{neg} population plotted in the myeloblast/monoblast area, although CD16, CD11b, and CD13 resulted mainly negative or occasionally dim (Fig. 4A). Mature and immature monocyte markers CD36 and CD115 were not expressed in *Pop#8*. CD33, CD38, and HLA-DR were detected, whereas costimulatory proteins CD80 and CD86 were not present (Table 3B).

CD64^{bright}CD31^{bright}CD14^{neg} as well as Lin^{neg}CD31^{bright}CD18$^{dim/int}$, sorted *Pop#8*, showed cytomorphological traits of the myeloblast/monoblast lineage. Conversely, mature elements of the monocyte/macrophage compartment were easily identified in CD64^{bright}CD31^{bright}CD14^{+} fraction (Fig. 4B). Clonogenic test revealed that *Pop#8* cells, despite their myeloblastic/monoblastic appearance, do not retain any hematopoietic colony-forming potential. In fact, after 14 days of culture in StemMACS HSC-CFU medium, only numerous clusters of <100 cells, were detectable. These clusters resulted constituted by aggregates of large rounded cells on top of few attached MPC-like cells. Rare uncolored hematopoietic colonies (median frequency of $6.2 \pm 2.0/10^6$ plated cells, $n = 4$) were instead detected applying CD64^{bright}CD31^{bright}CD14^{+}, those colonies were classified as derived from GM-CFUs or M-CFUs only (Fig. 4C) and probably were generated from CD14^{dim} myeloid precursors included in the CD14^{+} sort gate.

Phagocytic activity has been induced in Pop#8 cells cultured in the presence and also in the absence of hGM-CSF, as revealed by uptake of Indian ink particles (Supplementary Fig. S4).

CD64^{bright}CD31^{bright}CD14^{neg} sorted *Pop#8* were also able to generate MPCs, once cultured in DMEM/10%PhABS for 6 days (Fig. 4D, right panel). Those *Pop#8*-derived MPCs showed their mesangiogenic nature, differentiating in functional MSCs, which retain the adipogenic and osteogenic potential (Fig. 4E, right panels), and showing the ability to internalize Ac-LDL (Fig. 4F), as well as of sprouting angiogenesis from 3D spheroids once seeded on Matrigel (Fig. 4G.1). Cells from enzymatic digestion of sprouted spheroids generate CLT structures, in the secondary cultures on Matrigel (Fig. 4G.2). At a difference, CD64^{bright}CD31^{bright}CD14^{+} generated few loosely adherent MPC-like cells (Fig. 4D, left panel), unable to differentiate into functional MSCs once cultured in MesenPRO RS (Fig. 4E, left panels). Freshly sorted *Pop#8* plated directly in MesenPRO RS did not generate any culture (data not shown), in accordance with immunomagnetic separation results on CD31^{+} fraction (Supplementary Fig. S1D). Similarly, ex vivo isolated *Pop#8* failed to form cell aggregates during preparation of 3D spheroids (data not shown).

Gene expression analysis of *Pop#8* showed that neither *NESTIN* nor *SPP1* mRNA, highly expressed by cultured MPCs, were found. Conversely, *NANOG* and *OCT4A* were detected in *Pop#8* as well as in CD64^{bright}CD31^{bright}CD14^{+} fraction, with no significant difference with cultured MPCs. *PECAM* (CD31) expression resulted less than one log lower in *Pop#8* as compared with their CD14^{+} counterpart ($1.75 \pm 0.62 \times 10^{-1}$ and 1.37 ± 0.17, $P < 0.05$, respectively; $n = 3$, Supplementary Fig. S5).

Discussion

In this study, we describe the isolation by immunomagnetic fractioning of CD45^{low}CD64^{bright}CD31^{bright}CD14^{neg} subpopulation from adult hBM with the ability to generate MPCs in culture. Notably, CD45 and CD31 antigens are routinely included in the depletion cocktails to enrich for MSC progenitors [25]. Our results, therefore, indicate that MPCs and MSCs belong to different lineages in vivo.

The hypothesis that MPC and MSC progenitors are set apart in different bone marrow subpopulations was supported by the failure to isolate MSC-like cells directly from CD31^{+} fraction even under permissive culture conditions (gas-treated instead of hydrophobic plastic), as previously described in unfractionated hBM [12]. No MPC-like cells were obtained from CD105^{+} fractions suggesting also that the expression of endoglin in MPCs would be early induced in vitro.

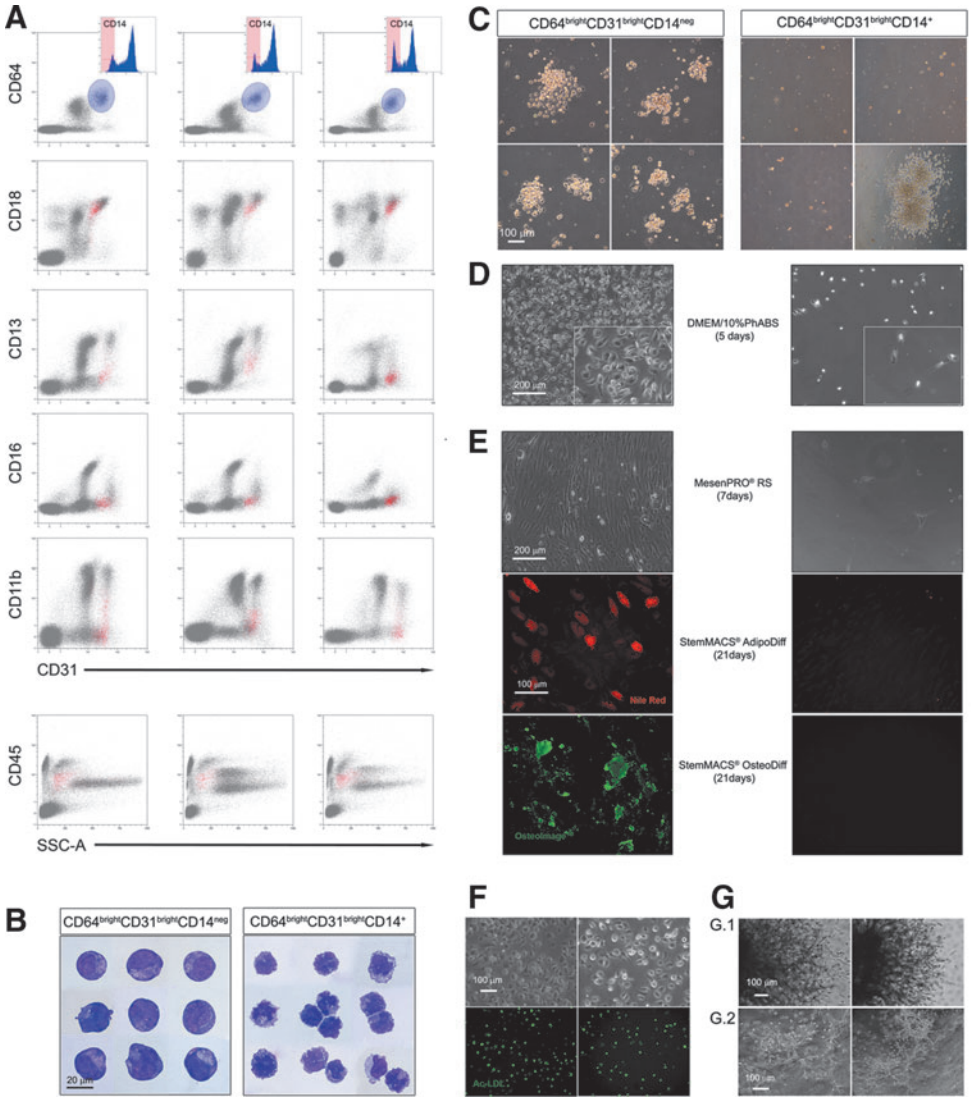

FIG. 4. *Pop#8* isolation by their unique CD64^{bright}CD31^{bright}CD14^{neg} phenotype. Gating events for bright expression of both CD31 and CD64 (*light blue gate*) most cells showed to be CD14^{+}. CD64^{bright}CD31^{bright}CD14^{neg} minor population plotted exclusively in the *R8* region of CD18 versus CD31 cytogram (*red dots*), confirming that this population was the *Pop#8* population (three representative samples are presented in **(A)**. CD45 was mildly expressed as well as CD13, CD16, and CD11b. CD64^{bright}CD31^{bright}CD14^{neg} appeared to be large cells with blast-like morphology, in sharp contrast with the monocytic morphology showed by the CD14^{+} counterpart **(B)**. Applying hematopoietic colony-forming assay, CD64^{bright}CD31^{bright}CD14^{neg} generated clusters of large cells above few adherent MPC-like cells not detected culturing the CD14^{+} counterpart, where GM- or M-CFUs were occasionally reported **(C)**. Consistently with Lin^{neg}CD31^{bright}CD18$^{dim/int}$, CD64^{bright}CD31^{bright}CD14^{neg} cells generated MPCs (*left panel*) **(D)** when cultured in DMEM/10%PhABS. Those MPCs rapidly differentiated into MSCs, which retained their adipogenic and osteogenic potential (*left panels*) **(E)**. The CD14^{+} counterpart failed to generate adherent cultures (*right panels*) **(D, E)**. *Pop#8*-derived MPCs were also capable of Ac-LDL uptake (*green* in **F**) and angiogenic sprouting **(G.1)** that primed the cells to form capillary tube-like structures **(G.2)**. Ac-LDL, acetylated low-density lipoprotein; GM-CFUs, granulocyte/macrophage colony-forming units; M-CFUs, macrophage colony-forming units.

Multicolor flow cytometry analysis of freshly isolated hBM-MNCs confirmed CD105^{+} and MSCA-1^{+} events to be confined in the *R1* (double negative) region of CD18 versus CD31 plot. Further characterization of the plot led to the identification of six different CD31^{+} subpopulations (*R3*, *R4*, *R5*, *R6*, *R7*, and *R8*; Fig. 2 and Table 1). The screening of FACS-sorted cell subpopulations for the ability to generate MPCs in culture allowed us to identify *R8* fraction as the putative candidate for MPC progenitor in vivo. We named the novel population ''*Pop#8*.'' Apparently, *Pop#8* seemed belonging to the myelocytic/monocytic lineage, and in details, these cells partially resemble precursors of monocytes and macrophages, considering their morphology, immunophenotype, and the ability to generate phagocytes. A genuine hematopoietic colony-forming potential has not been detected on *Pop#8*, however, it interestingly revealed signs of replication when culturing these cells in StemMACS HSC-CFU medium, which contains 30% of FBS, instead of the

expected mesengenic differentiation [12,13]. This could be explained by a possible effect of the hematopoietic growth factors, as stem cell factors (SCF) and GM-CSF contained at high doses in the semisolid medium, on *Pop#8* cells.

Quantitative analysis showed the frequency of *Pop#8* (1.3%) to be consistent with reported frequency (0.9%) of cultured MPCs from hBM-MNCs [13]. MPCs derived from culturing *Pop#8* in PhABS-containing medium resulted undistinguishable from MPCs from unfractionated hBM-MNCs. They showed the expected mesengenic and angiogenic differentiation potential, giving rise, respectively, to MSCs matching the ISCT criteria [26] and retaining the adipogenic/osteogenic differentiation capability, as well as of sprouting angiogenesis.

Therefore, we were able to obtain MSCs in vitro starting from the CD31^{+} compartment, which is usually excluded from the studies on prospective isolation of in vivo MSC progenitors. Further *Pop#8* characterization revealed CD45 to be mildly expressed, whereas most of the antigens feasible for prospective isolation of MSCs from bone marrow [11] remained unexpressed. In particular, the lack of CD146 expression on ex vivo *Pop#8,* similar to what is reported for the in vitro MPCs, suggests that this cell population is distinct from the CD146^{bright} clonogenic progenitor, residing in the subendothelial layer of sinusoids, identified by Sacchetti et al. [27]. Thus, *Pop#8* could represent an inducible postnatal BM stromal progenitor that should be considered distinct from the determined self-renewing, multipotent progenitors for skeletal tissue, recently described as SSCs [28]. This is also suggested by the evidence that CD146^{neg} *Pop#8* could be easily induced in vitro into a CD146^{dim} MSC-like osteogenic cell strain (Fig. 3E), where the low expression of CD146 results in accordance to the expression levels reported on the ''non-stem'' osteogenic cell populations [27].

Most of the information available on MSC biology is derived from in vitro studies making it difficult to determine the primary cells of origin. A multitude of ex vivo MSC progenitors, representing distinct and sometimes mutually exclusive populations, has been identified from different tissues [29,30]. In particular, for hBM-derived MSCs strong evidence indicates that the fibroblastoid colonies originally described by Friedenstein et al. [31] originated from the CD146^{+} pericytic population residing in the subendothelial layer of bone marrow sinusoids [27,32,33]. More recently, in vivo MSC progenitors were localized in the trabecular bone lining CD271^{+}CD146^{neg} cell population as well [34]. Stromal reticular cells also were shown to retain MSC-like adipogenic/osteogenic potential [35].

Therefore, cells with different immunophenotypes can generate MSCs in the perivascular, in the endosteum, as well as in the stromal bone marrow compartments. The search for the MSC progenitor is turning into a search for various MSC progenitors, with their mutual relationship still to be clarified. In this scenario, our results indicate that MSC-like cells can be indirectly propagated also from a distinctive CD146^{neg}CD271^{neg}CD31^{bright}CD45^{low} population; this also represents a peculiar feature of *Pop#8*. In fact, this cell population, conversely to other mesengenic or angiogenic progenitor cells isolated, showed neither CFU-F nor CFU-Hill properties when directly cultured in differentiating conditions, and only after induction in MPCs demonstrates its mesangiogenic potential.

Thus, in our hands *Pop#8* represents the exclusive primary ex vivo precursor of MPCs that were shown to be in vitro progenitor of both mesenchymal and endothelial lineages [12,13]. This suggests a possible functional role of *Pop#8* in the local maintaining of the HSC supporting microenvironment that include remodeling of both the microvascular plexus and the stromal compartment [36,37], acting as inducible progenitor, as hypothesized above. The precise anatomical localization of *Pop#8* and serial transplantation experiments are necessary to clarify these aspects, and will be the object of future studies.

The demonstration that nestin^{+} perivascular MSCs are crucial in maintaining bone marrow HSC pool in a steady state [38] casts new light on the role of this intermediate filament protein previously associated to central nervous system development [39,40] and malignancy [41]. In murine and human bone marrow, nestin^{+} MSCs in close contact with HSCs at perivascular locations, in the endosteum and in the stroma, were found expressing HSC maintenance genes as *CXCL12*, *SCF*, and *SPP1* [42]. Moreover, *NESTIN* expression was associated to angiogenesis in proliferating endothelial progenitors at a difference with mature endothelial cells [43]. Induction of *SPP1* expression was also reported in the vascular remodeling process [44,45] and specifically in *neointima* formation [46].

Therefore, nestin and osteopontin appear to be good candidate markers for both the mesengenic and angiogenic remodeling processes. The idea is intriguing, in particular regard to tissues which are physiologically highly remodeled, like bone marrow. Notably, we found *NESTIN* and *SPP1* to be consistently upregulated when *Pop#8* were cultured to generate MPCs, further corroborating the hypothesis of a *Pop#8* role as in vivo progenitor of the different cell populations involved in bone marrow microenvironment remodeling.

Moreover, the discovery of *Pop#8* in hBM-MNCs strongly supports the idea that most of the controversies regarding culture-expanded MSCs could be the consequence of different culture conditions that select or promote particular subpopulations of precursors [47]. *Pop#8* resulted from two to three logs more frequent than other putative MSC progenitors reported in hBM-MNCs, making it reasonable that specific culture systems (ie, different batches of human or bovine sera) could affect the percentage of coisolated MPCs. We believe the heterogeneous composition of cultures, including subpopulations of MPCs and MSCs to be responsible for the controversial data regarding angiogenic potential of MSC cultures, as previously reported [48].

In conclusion, in this study, we demonstrated that MPCs arise from a unique novel CD45^{low}CD64^{bright}CD31^{bright}CD14^{neg} human bone marrow subpopulation (*Pop#8*), whose identification could represent a significant contribution to the debate on MSC in vivo progenitors. Further studies are needed to localize *Pop#8* in vivo and to define its role on the homeostasis and pathology of bone marrow microenvironment.

Acknowledgment

Regione Toscana supported this work under ''Bando Salute'' grant.

Author Disclosure Statement

No competing financial interests exist.

References

1. Si YL, YL Zhao, HJ Hao, XB Fu and WD Han. (2011). MSCs: biological characteristics, clinical applications and their outstanding concerns. Ageing Res Rev 10:93–103.
2. Madrigal M, KS Rao and NH Riordan. (2014). A review of therapeutic effects of mesenchymal stem cell secretions and induction of secretory modification by different culture methods. J Transl Med 12:260.
3. Sharma RR, K Pollock, A Hubel and D McKenna. (2014). Mesenchymal stem or stromal cells: a review of clinical applications and manufacturing practices. Transfusion 54:1418–1437.
4. Dimarino AM, AI Caplan and TL Bonfield. (2013). Mesenchymal stem cells in tissue repair. Front Immunol 4:201.
5. Ankrum J and JM Karp. (2010). Mesenchymal stem cell therapy: two steps forward, one step back. Trends Mol Med 16:203–209.
6. Wang S, X Qu and RC Zhao. (2012). Clinical applications of mesenchymal stem cells. J Hematol Oncol 5:19.
7. Farini A, C Sitzia, S Erratico, M Meregalli and Y Torrente. (2014). Clinical applications of mesenchymal stem cells in chronic diseases. Stem Cells Int 2014:306573.
8. Delorme B, J Ringe, N Gallay, Y Le Vern, D Kerboeuf, C Jorgensen, P Rosset, L Sensebe, P Layrolle, T Haupl and P Charbord. (2008). Specific plasma membrane protein phenotype of culture-amplified and native human bone marrow mesenchymal stem cells. Blood 111:2631–2635.
9. Harichandan A and HJ Buhring. (2011). Prospective isolation of human MSC. Best Pract Res Clin Haematol 24:25–36.
10. Matsuoka Y, R Nakatsuka, K Sumide, H Kawamura, M Takahashi, T Fujioka, Y Uemura, H Asano, Y Sasaki, et al. (2015). Prospectively isolated human bone marrow cell-derived MSCs support primitive human CD34-negative hematopoietic stem cells. Stem Cells 33:1554–1565.
11. Lv FJ, RS Tuan, KM Cheung and VY Leung. (2014). Concise review: the surface markers and identity of human mesenchymal stem cells. Stem Cells 32:1408–1419.
12. Petrini M, S Pacini, L Trombi, R Fazzi, M Montali, S Ikehara and NG Abraham. (2009). Identification and purification of mesodermal progenitor cells from human adult bone marrow. Stem Cells Dev 18:857–866.
13. Trombi L, S Pacini, M Montali, R Fazzi, F Chiellini, S Ikehara and M Petrini. (2009). Selective culture of mesodermal progenitor cells. Stem Cells Dev 18:1227–1234.
14. Frith J and P Genever. (2008). Transcriptional control of mesenchymal stem cell differentiation. Transfus Med Hemother 35:216–227.
15. Augello A and C De Bari. (2010). The regulation of differentiation in mesenchymal stem cells. Hum Gene Ther 21:1226–1238.
16. Pacini S, V Carnicelli, L Trombi, M Montali, R Fazzi, E Lazzarini, S Giannotti and M Petrini. (2010). Constitutive expression of pluripotency-associated genes in mesodermal progenitor cells (MPCs). PLoS One 5:e9861.
17. Pacini S, R Fazzi, M Montali, V Carnicelli, E Lazzarini and M Petrini. (2013). Specific integrin expression is associated with podosome-like structures on mesodermal progenitor cells. Stem Cells Dev 22:1830–1838.
18. Fazzi R, S Pacini, V Carnicelli, L Trombi, M Montali, E Lazzarini and M Petrini. (2011). Mesodermal progenitor cells (MPCs) differentiate into mesenchymal stromal cells (MSCs) by activation of Wnt5/calmodulin signalling pathway. PLoS One 6:e25600.
19. Montali M, S Barachini, S Pacini, FM Panvini and M Petrini. (2016). Isolating mesangiogenic progenitor cells (MPCs) from human bone marrow. J Vis Exp. [Epub ahead of print]; e54225, DOI: 10.3791/54225(2016).
20. Del Duca D, T Werbowetski and RF Del Maestro. (2004). Spheroid preparation from hanging drops: characterization of a model of brain tumor invasion. J Neurooncol 67:295–303.
21. Foty R. (2011). A simple hanging drop cell culture protocol for generation of 3D spheroids. J Vis Exp pii:2720.
22. DeCicco-Skinner KL, GH Henry, C Cataisson, T Tabib, JC Gwilliam, NJ Watson, EM Bullwinkle, L Falkenburg, RC O'Neill, A Morin and JS Wiest. (2014). Endothelial cell tube formation assay for the in vitro study of angiogenesis. J Vis Exp e51312.
23. Graham GS. (1918). Benzidine as a peroxidase reagent for blood smears and tissues. J Med Res 39:15–24.1.
24. Livak KJ and TD Schmittgen. (2001). Analysis of relative gene expression data using real-time quantitative PCR and the 2(-Delta Delta C(T)) method. Methods 25:402–408.
25. Modder UI, MM Roforth, KM Nicks, JM Peterson, LK McCready, DG Monroe and S Khosla. (2012). Characterization of mesenchymal progenitor cells isolated from human bone marrow by negative selection. Bone 50:804–810.
26. Dominici M, K Le Blanc, I Mueller, I Slaper-Cortenbach, F Marini, D Krause, R Deans, A Keating, D Prockop and E Horwitz. (2006). Minimal criteria for defining multipotent mesenchymal stromal cells. The International Society for Cellular Therapy position statement. Cytotherapy 8:315–317.
27. Sacchetti B, A Funari, S Michienzi, S Di Cesare, S Piersanti, I Saggio, E Tagliafico, S Ferrari, PG Robey, M Riminucci and P Bianco. (2007). Self-renewing osteoprogenitors in bone marrow sinusoids can organize a hematopoietic microenvironment. Cell 131:324–336.
28. Bianco P and PG Robey. (2015). Skeletal stem cells. Development 142:1023–1027.
29. Buhring HJ, VL Battula, S Treml, B Schewe, L Kanz and W Vogel. (2007). Novel markers for the prospective isolation of human MSC. Ann N Y Acad Sci 1106:262–271.
30. Mabuchi Y, DD Houlihan, C Akazawa, H Okano and Y Matsuzaki. (2013). Prospective isolation of murine and human bone marrow mesenchymal stem cells based on surface markers. Stem Cells Int 2013:507301.
31. Friedenstein AJ, KV Petrakova, AI Kurolesova and GP Frolova. (1968). Heterotopic of bone marrow. Analysis of precursor cells for osteogenic and hematopoietic tissues. Transplantation 6:230–247.
32. Farrington-Rock C, NJ Crofts, MJ Doherty, BA Ashton, C Griffin-Jones and AE Canfield. (2004). Chondrogenic and adipogenic potential of microvascular pericytes. Circulation 110:2226–2232.
33. Brighton CT, DG Lorich, R Kupcha, TM Reilly, AR Jones and RA Woodbury, 2nd. (1992). The pericyte as a possible osteoblast progenitor cell. Clin Orthop Relat Res 287–299.
34. Tormin A, O Li, JC Brune, S Walsh, B Schutz, M Ehinger, N Ditzel, M Kassem and S Scheding. (2011). CD146 expression on primary nonhematopoietic bone marrow stem cells is correlated with in situ localization. Blood 117:5067–5077.
35. Omatsu Y, T Sugiyama, H Kohara, G Kondoh, N Fujii, K Kohno and T Nagasawa. (2010). The essential functions of adipo-osteogenic progenitors as the hematopoietic stem and progenitor cell niche. Immunity 33:387–399.
36. Doan PL and JP Chute. (2012). The vascular niche: home for normal and malignant hematopoietic stem cells. Leukemia 26:54–62.

37. Mendez-Ferrer S, DT Scadden and A Sanchez-Aguilera. (2015). Bone marrow stem cells: current and emerging concepts. Ann N Y Acad Sci 1335:32–44.
38. Mendez-Ferrer S, TV Michurina, F Ferraro, AR Mazloom, BD Macarthur, SA Lira, DT Scadden, A Ma'ayan, GN Enikolopov and PS Frenette. (2010). Mesenchymal and haematopoietic stem cells form a unique bone marrow niche. Nature 466:829–834.
39. Dahlstrand J, M Lardelli and U Lendahl. (1995). Nestin mRNA expression correlates with the central nervous system progenitor cell state in many, but not all, regions of developing central nervous system. Brain Res Dev Brain Res 84:109–129.
40. Lendahl U, LB Zimmerman and RD McKay. (1990). CNS stem cells express a new class of intermediate filament protein. Cell 60:585–595.
41. Tohyama T, VM Lee, LB Rorke, M Marvin, RD McKay and JQ Trojanowski. (1992). Nestin expression in embryonic human neuroepithelium and in human neuroepithelial tumor cells. Lab Invest 66:303–313.
42. Pinho S, J Lacombe, M Hanoun, T Mizoguchi, I Bruns, Y Kunisaki and PS Frenette. (2013). PDGFRalpha and CD51 mark human nestin+ sphere-forming mesenchymal stem cells capable of hematopoietic progenitor cell expansion. J Exp Med 210:1351–1367.
43. Matsuda Y, M Hagio and T Ishiwata. (2013). Nestin: a novel angiogenesis marker and possible target for tumor angiogenesis. World J Gastroenterol 19:42–48.
44. Infanger M, M Shakibaei, P Kossmehl, SM Hollenberg, J Grosse, S Faramarzi, G Schulze-Tanzil, M Paul and D Grimm. (2005). Intraluminal application of vascular endothelial growth factor enhances healing of microvascular anastomosis in a rat model. J Vasc Res 42: 202–213.
45. Leen LL, C Filipe, A Billon, B Garmy-Susini, S Jalvy, F Robbesyn, D Daret, C Allieres, SR Rittling, et al. (2008). Estrogen-stimulated endothelial repair requires osteopontin. Arterioscler Thromb Vasc Biol 28:2131–2136.
46. Li XD, J Chen, CC Ruan, DL Zhu and PJ Gao. (2012). Vascular endothelial growth factor-induced osteopontin expression mediates vascular inflammation and neointima formation via Flt-1 in adventitial fibroblasts. Arterioscler Thromb Vasc Biol 32:2250–2258.
47. Pacini S. (2014). Deterministic and stochastic approaches in the clinical application of mesenchymal stromal cells (MSCs). Front Cell Dev Biol 2:50.
48. Pacini S and I Petrini. (2014). Are MSCs angiogenic cells? New insights on human nestin-positive bone marrow-derived multipotent cells. Front Cell Dev Biol 2:20.

Address correspondence to:
Dr. Simone Pacini
Hematology Division
Department of Clinical and Experimental Medicine
University of Pisa
Via Roma 56
Pisa 56126
Italy

E-mail: simone.pacini@do.unipi.it

Received for publication November 3, 2015
Accepted after revision March 14, 2016
Prepublished on Liebert Instant Online March 15, 2016